Research Article

Hongmin Li, Jingting Liu*, Songying Chen*, and Wei Lv

Numerical investigation of ozone decomposition by self-excited oscillation cavitation jet

https://doi.org/10.1515/phys-2022-0005
received August 18, 2021; accepted January 10, 2022

Abstract: Extreme environmental changes caused by the cavitation bubble collapse, such as high pressure, high temperature and the microjet, will cause pyrolysis reaction at the gas and liquid interface inside the bubble. Self-excited pulsed cavitation jet has an instantaneous strong pulse pressure, which leads to local hot spots surrounding the cavitation bubbles. The generation of strong oxidizing free radicals promotes easy ozone conversion into oxygen. Numerical simulations were conducted for ozone decomposition by cavitation jet. Three groups of different collision angles were applied to compare and analyze the ozone degradation reaction. Results showed that the collision angle has a certain influence on the chemical reaction intensity, the degradation of ozone, and oxygen production. At the collision angle of 180°, the chemical reaction was the most violent, with ozone degradation and oxygen production at the highest level, followed by 120° and lowest at 90°.

Keywords: self-excited pulsed cavitation jet, ozone decomposition, collision angle, water disinfection

1 Introduction

The self-excited pulsed cavitation jet is a kind of high-efficiency pulsed jet [1]. The continuous jet flow produces self-excited oscillation through a special structure and transforms into an oscillating pulse jet with a stronger impact and shock effect. Meanwhile, cavitation bubbles occur as a result of sudden pressure change during the jet process. Based on the operating principle of a self-excited cavitation nozzle [2], the organ nozzle could be designed by changing the structure size to change the vibration frequency. A large number of results [3] show that the frequency of the self-excited vibration resonance could improve the cleaning capability of the nozzle to the maximum extent.

With the development of computational fluid dynamics (CFDs), the fluent platform has been applied to conduct a variety of comparative analyses and numerical simulations of self-excitation pulse cavitation jets [4,5]. Hu [6] analyzed the waveform and frequency domain characteristics of a self-excited pulse cavitation jet. Gravity factors play an important role in the changing of the flow field of the nozzle cavity. Xiang *et al.* [7] studied the mixing processes of different linear gasoline with rotary jet mixer (RJM) (based on the rotary jet mixing system) using numerical simulation. The radial velocity attenuation curve of the horizontal nozzle and velocity contours of different mixed-flow fields are discussed. A two-dimensional unsteady numerical simulations with mixture model are adopted to investigate the influence of nozzle structure and environmental parameters on the effect of self-excited oscillation pulsed with a nozzle with an upper diameter of 6.68 mm [8]. Moholkar [9] proposed a cavitation model suitable for turbulence intensity. Compared with the linear pressure distribution model, the collapse process of

* **Corresponding author: Jingting Liu,** School of Mechanical Engineering, Shandong University, Jinan 250061, China; Key Laboratory of High-efficiency and Clean Mechanical Manufacture, Ministry of Education, Jinan 250061, China; National Demonstration Center for Experimental Mechanical Engineering Education at Shandong University, Jinan 250061, China, e-mail: liujingting@sdu.edu.cn
* **Corresponding author: Songying Chen,** School of Mechanical Engineering, Shandong University, Jinan 250061, China; Key Laboratory of High-efficiency and Clean Mechanical Manufacture, Ministry of Education, Jinan 250061, China; National Demonstration Center for Experimental Mechanical Engineering Education at Shandong University, Jinan 250061, China, e-mail: chensy66@sdu.edu.cn
Hongmin Li, Wei Lv: School of Mechanical Engineering, Shandong University, Jinan 250061, China; Key Laboratory of High-efficiency and Clean Mechanical Manufacture, Ministry of Education, Jinan 250061, China; National Demonstration Center for Experimental Mechanical Engineering Education at Shandong University, Jinan 250061, China

cavitation bubbles in the calculation model after the introduction of turbulence pulsation term is more drastic and the numerical simulation results are more reasonable.

With the gradual progress of the economy, water pollution has become more and more rampant, which has become one of the inevitable topics and attracted the attention of lots of people. Jet cavitation technology [10] has made great progress in the field of water purification due to its simple structure and rapid development. Since the collapse of cavitation bubbles can cause instantaneous local high temperature and high pressure to accelerate the efficiency of a chemical reaction. Recently, based on the environmental conditions, submerged cavitation water jet were constructed to generate cavitation, and multiple degradation measures were taken for industrial wastewater containing *p*-nitrophenol [11]. Experimental data show that compared with the ultrasonic cavitation method, the energy utilization rate has been improved by several orders of magnitude, and the efficiency has been greatly improved. Jyoti and Pandit [12] discussed the sterilization effect of the energy of bubble collapse in the cavitation process on the disinfection of drinking water. Compared with the previous non-chemical water treatment technology, hydrodynamic cavitation [13] is an energy-saving and economic water treatment technology with huge economic benefits. A liquid sentinel cavitation reactor was used to degrade sewage pollutants [14]. When the sewage passes through a single pipe reactor, a high-pressure and high-speed cavitation jet hits the leaf margin choke. Cavitation phenomenon occurs and huge energy generates at the moment of cavitation collapse, which speeds up the chemical reaction and the mixture of reactants. Combined with benton method, the removal rate of industrial wastewater with initial TOC 14,000 mg/L can reach 80%.

Ozone water treatment is widely respected in water purification because of its strong oxidation capacity and no secondary pollutants [15]. It has a long history of application. As early as the beginning of the last century, the first water plant in Nice, France, adopted ozonation technology for water quality treatment and ozonation water treatment technology has drawn public attention since then [16]. Staehelin and Hoigne [17] chose to analyze and compare the decomposition behavior of ozone in different water samples and conducted experimental research. The corresponding decomposition kinetic principle is summarized, and it is proved that many active radicals would be generated when ozone is degraded in an aqueous solution. It is a chain reaction process, which provides a theoretical basis for the subsequent treatment of water by ozone.

Gracia *et al.* [18] first studied that the addition of Mn^{2+} as a catalyst accelerated the degradation of organic and inorganic substances in ozonation of water. There is an effective reduction in the content of aromatic, aldehydes, phenol and other organic compounds, and improvement in the water quality. Mainardis *et al.* [19] found that compared with bleaching water, the chemical oxygen demand (COD) removal effect of ozone in processing water was more obvious, up to 60%. According to literature, compared with other biological technologies, the decomposition rate of COD in water could reach 81% after the treatment of pulp and paper mixed industrial wastewater, which confirmed the significant role of ozone in the water treatment field.

Zhai *et al.* [20] put forward the hydraulic cavitation technology and ozone oxidation technique combined sewage treatment and investigated separately the hydraulic cavitation and ozone degradation associated with the degradation of water COD removal effect. Results show that hydraulic cavitation combined with ozone degradation effects are better than the two separate degradation processes. Chang *et al.* [21] used a rotating packed bed (RPB) as the chemical reactor. Meanwhile, the ozone oxidation process was used to degrade the effluent from the first stage biochemical tank of Orchid carbon wastewater. The effects of ozone concentration, RPB rotating speed, gas–liquid ratio, pH of wastewater, wastewater temperature, and RPB reaction level on industrial wastewater treatment and ozone utilization were investigated, which provided certain theoretical data for water purification. Yang *et al.* [22] applied hydraulic cavitation, ozone, positive pressure cavitation combined with ozone, and suction cavitation combined with ozone to degrade production of wastewater. It is found that application of hydraulic cavitation and ozone separately for COD degradation had little effect, and COD removal efficiency after the two processes were combined can be as high as 80%.

Ozone water treatment technology has been widely applied and promoted [23] in the field of water treatment due to its advantages such as low cost, fast reaction rate, and non-toxicity of by-products. In this article, a cavitation jet is selected to be combined with ozone decomposition. Cavitation can promote ozone decomposition; meanwhile, jet oxygenation and bactericidal treatment are carried out for the water body, which is a good choice for the development of water body purification [24].

2 Model and methods

2.1 Geometric modeling

The structural parameters of self-excited pulsed cavitating jet nozzle [25] are mainly composed of upper nozzle of diameter d_1, lower nozzle of diameter d_2, cavity

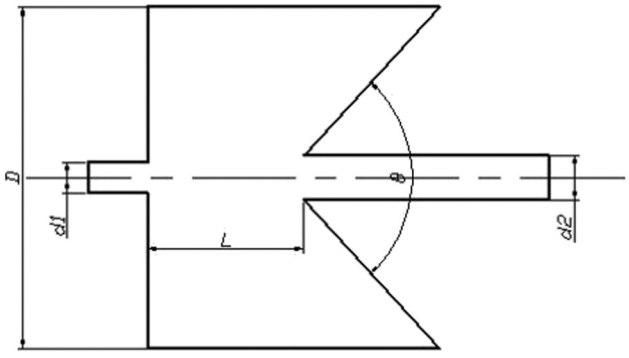

Figure 1: Outline of the nozzle.

length of L, cavity diameter of D, and collision angle θ, as shown in Figure 1.

The inner cavity of the nozzle is symmetrical, and the ozone inlet is set above the nozzle. For the convenience of numerical calculation, it is simplified into a two-dimensional axisymmetric model, as shown in Figure 2.

2.2 Boundary and initial conditions

In the numerical simulations, the upper nozzle is set as the pressure inlet located in the middle of the left plane of the chamber. And the inlet pressure is 1.5 MPa. The lower nozzle is set as the pressure outlet located in the middle position on the right end face of the chamber, and the outlet pressure is 0.1 MPa. The ozone inlet position is placed 30 mm from the left ventricular surface on the upper side, and the mass flow rate is 20 g/h. The outer wall is set as the no-slipping wall.

The physicochemical properties of ozone and water in this study are shown in Table 1.

2.3 Numerical methods

CFD method can solve the complex and changeable fluid motion equation that cannot be solved by theoretical analysis, and it is more economical and practical compared with the experimental method. However, as an approximate solution method, the accuracy of numerical results is affected by many factors [26,27]. The number and quality of mesh and time step are the factors that cannot be ignored in the numerical simulation, so it is necessary to eliminate such errors as much as possible to ensure the accuracy of the simulation.

In this study, four sets of grids with different densities ranging from 13,000 to 890,000 were set, and the growth ratio of adjacent density grids was 4. Specific parameter settings are shown in Table 2. As shown in Figure 3, the local grid of nozzle inlet and ozone inlet as shown in Figure 2 is selected as the detailed display for convenience. In Figure 3(a)–(d), four groups of grid density diagrams from sparse to dense for inlets are shown, respectively [28]. In the process of grid independence verification, point A in the chamber of the nozzle cavity is selected as the reference value. It can be found from Figure 4 that with the increase in grid number, the liquid velocity ratio v/v_0 at point A has stopped changing, where v_0 is eight times the velocity at the standardized grid at point A, and the calculated results tend to be stable. At the same time, when the number of grids is

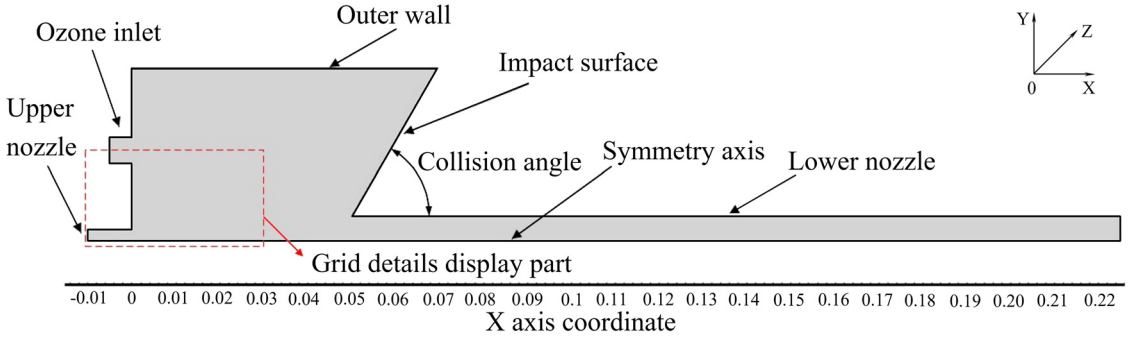

Figure 2: Schematic diagram of a two-dimensional axisymmetric model.

Table 1: Physicochemical properties of ozone and water

	Density (kg/m^3)	Dynamic viscosity (Pa s)	Operating temperature (°C)	Mixing length limit (mm)
O_3	1.0	1.72×10^{-5}	20	$L \leq 50$
H_2O	998.2	0.8984×10^{-3}	20	

Table 2: Parameter settings for grid independence verification

Grid group	Standardized grid scale	Grid number	Liquid velocity ratio v/v_0
1	8	13,000	1.010
2	4	53,000	1.035
3	2	220,000	1.065
4	1	890,000	1.040

more than 220,000, the mesh stretching ratio is 1.02, which can well meet the requirements of grid independence. At the same time, adopting the grid density of group 4 requires a lot of time and wastes computing resources. After comprehensive consideration, group 3 in Figure 3(c), namely 220,000 grids, was finally selected for numerical simulations. And the time step $\Delta t = 5 \times 10^{-6}$ s was selected. Boundary conditions were set as pressure inlet and pressure outlet. Ozone inlet boundary conditions were set as mass-flow inlet, 20 g/h.

In the numerical process, the Navier–Stokes equation is used to describe the pulse jet:

$$\frac{\partial(\rho\vec{u})}{\partial t} + \nabla(\rho\vec{u}\vec{u}) = -\nabla p + \nabla\tau + \rho\vec{g} + \vec{F}, \quad (1)$$

where t is the time, u is the speed, ρ is the mixing density, p is the static pressure, τ is the stress tensor, and $\rho\vec{g}$ and $\vec{F}$ are, respectively, the gravitational body force and the external body force. The RNG k-epsilon model and the mixture multiphase model are adopted to resolve the pulsed cavitation jet flow field. The Schnerr–Sauer cavitation model

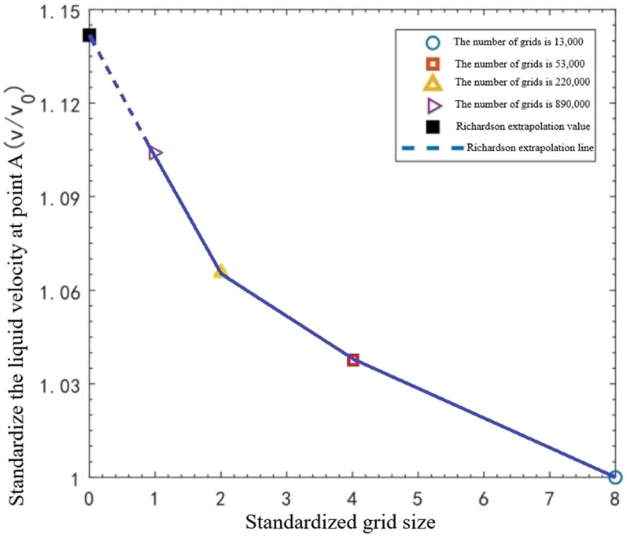

Figure 4: Liquid velocity at measuring point A with different grid densities v/v_0.

[29] modified by introducing the shear stress term and turbulent kinetic energy term is adopted in the numerical simulations.

$$R_e = \frac{\rho_v\rho_l}{\rho}\alpha_v(1-\alpha_v)\frac{3}{R_B}\sqrt{\frac{2}{3}\frac{(p_v' - p_l)}{\rho_l}}, \quad (2)$$

$$p_v' = p_v + 0.195\rho k + \frac{\sqrt{2}}{2}(\mu + \mu_t)\left(\frac{\partial u}{\partial y} + \frac{\partial v}{\partial x}\right), \quad (3)$$

where k is the turbulent kinetic energy, μ and μ_t are the dynamic viscosity and the turbulent viscosity of the

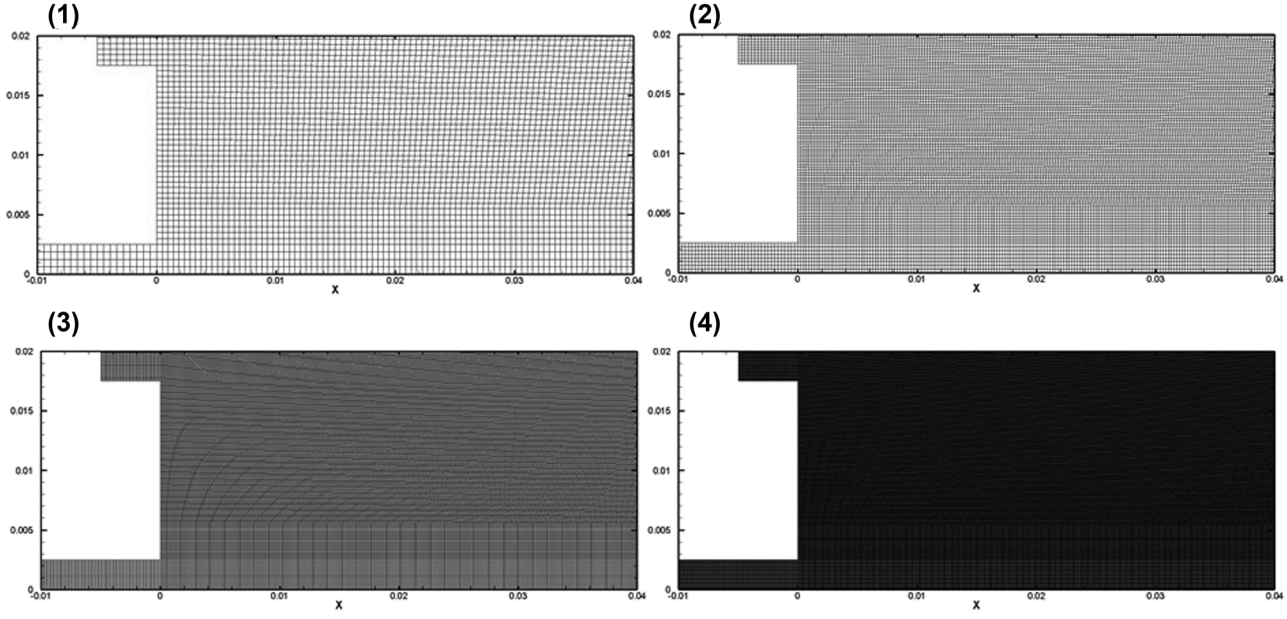

Figure 3: Different mesh densities at nozzle inlet.

mixture, respectively. The local saturation vapor is modified with the turbulent kinetic energy term $0.195\rho k$ and the shear stress term $\frac{\sqrt{2}}{2}(\mu + \mu_t)\left(\frac{\partial u}{\partial y} + \frac{\partial v}{\partial x}\right)$ is that the formation of vapor in the self-excited pulsed jet nozzle is related to the shear stress and the pressure oscillation arisen from the turbulent kinetic energy.

In the process of self-excited pulsed cavitation jet, the collapse of the cavitation bubble will generate instantaneous pulse pressure [30]. Meanwhile, local hot spots will be formed around the cavitation bubbles, and extreme phenomena such as high pressure, high temperature, and micro-jet will occur. As a result, pyrolysis reaction occurs at the gas–liquid interface, and strong oxidizing free radicals are generated [26]. The environmental changes during cavitation bubble collapse promote the decomposition of ozone, and the existence of strong oxidizing free radicals also accelerates the reaction.

The decomposition of ozone molecules usually results from the dissociation of ozone generated by the collision of O_3 molecules with O_2 molecules or atomic O. In the decomposition process of self-excited pulsed cavitation jet ozone, the excitation of electrons or vibration dynamics in O_3 or O molecules and the excited O atoms can be ignored. Therefore, we consider the following reactions in this study:

$$O_3 + O_2 \rightarrow 2O_2 + O, \ k_1, \tag{4}$$

$$O_3 + O \rightarrow 2O_2, \ k_2, \tag{5}$$

where k_1 is the decomposition rate of the interaction of O_3 and O_2, and k_2 is the chemical reaction rate of the interaction between O_3 molecule and O atoms.

In combination with equations (4) and (5), the total chemical reaction rate k can be defined as

$$k = k_1(1 - \alpha) + k_2\alpha, \tag{6}$$

where α and $(1 - \alpha)$, respectively, represent the mixing ratio of O atoms and O_2 molecules. The value of k_1 and k_2 can be confirmed from the formula given below [27]

$$k_1 = 7.82 \times 10^{-14} \exp\left[-\frac{9{,}300}{T}\right] \ \text{cm}^3/\text{s}, \tag{7}$$

$$k_2 = 7.52 \times 10^{-12} \exp\left[-\frac{2{,}080}{T}\right] \ \text{cm}^3/\text{s}, \tag{8}$$

where T is temperature. The values of k_1 and k_2 are consistent with the results obtained by Eliasson [31] and Kogelschatz *et al.* [32].

It can be seen from equation (7) that the combination of O_3 and O_2 is an endothermic reaction. The process of reaction is endothermic with the change in enthalpy, and its enthalpy value is $\Delta H_1 = 106.5$ kJ/mol. In equation (8), the combination of O_3 and O atoms is exothermic with the change in enthalpy, and its enthalpy value is $\Delta H_2 = -391.9$ kJ/mol. Due to $\Delta H = \Delta H_1 + \Delta H_2 = -285.5$ kJ/mol, the whole chemical reaction process of ozone decomposition is an exothermic reaction. With the increase in temperature, the reaction rate of ozone decomposition is accelerated.

The ozone decomposition reaction in the chamber of the self-excited pulse cavity is carried by the jet stream, and there is excess water in the whole process. Considering that the decomposition of ozone in an aqueous solution involves a series of reactions involving free radicals, the chemical reaction equation can be abbreviated as:

$$2O_3 + H_2O_{(l)} \rightarrow 3O_2 + H_2O_{(g)}. \tag{9}$$

Species transport model is utilized to explore the decomposition of ozone according to the above chemical reactions. The phase of ozone is defined as the mixture template in this study, involving ozone gas, oxygen, and vapor.

2.4 Three-line method analysis

The position of the ozone inlet is discussed. The three-line method of evaluation in data processing of CFD is widely used and has higher reliability and accuracy. As shown in Figure 5, in the cloud map of ozone volume distribution of the flow field inside the self-excited pulse chamber, the point of the vortex center is taken as the base point. A line parallel to the impact surface is selected as Line 1. Line 2 parallel is to the central axis, and Line 3 is perpendicular to the central axis. The ozone gas phase volume fraction distribution on these three lines was used to determine the optimal location of the ozone inlet. This analysis can be more intuitive to use

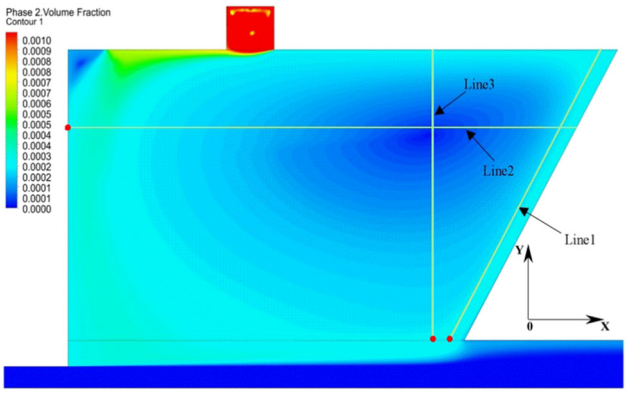

Figure 5: Schematic diagram of the three-line method.

data analysis results, comparing simple knowledge chart analysis.

The changes in ozone velocity with the length of three lines are shown in Figure 6. The starting points of three lines are marked with red dots in Figure 5. The trend of velocity variation on the three lines is different, but the formation of regions with small velocities has the same cause. The decrease in velocity results from ozone decomposition under the effect of cavitation. Figure 7 shows the changes in ozone gas phase volume fraction based on the three-line method. The four curves A, B, C, and D in the figure represent the ozone volume fraction distribution when the ozone inlet is at the left and the interval with the central axis is 15, 20, 25, and 27.5 mm. E, F, G, and H represent the ozone volume fraction distribution cloud map at the upper side of the entrance and the distance to the left side of the chamber is 20, 30, 40, and 55 mm, respectively. Combined with the curves of Line 1, Line 2, and Line 3, it can be seen that the ozone distribution content of curve H is always the highest, indicating that the position 55 mm to the left of the chamber is the best design. However, the position 55 mm to the left of the chamber wall is too close to the impact wall, and the design requirements cannot be met when the impact angle changes. While the closer the entrance position is to the impact surface, the more difficult the processing is. So, the design of this position is abandoned. Meanwhile, the inlet position 30 mm to the left of the chamber is located in the middle position on the upper side of the chamber, meeting the requirements of various collision angles. The curve of F corresponding to the position 30 mm to the left of the chamber is better at meeting the requirements. Therefore, the ozone inlet location is finally determined to be 30 mm to the left of the upper side for the following chemical reaction analysis and simulation.

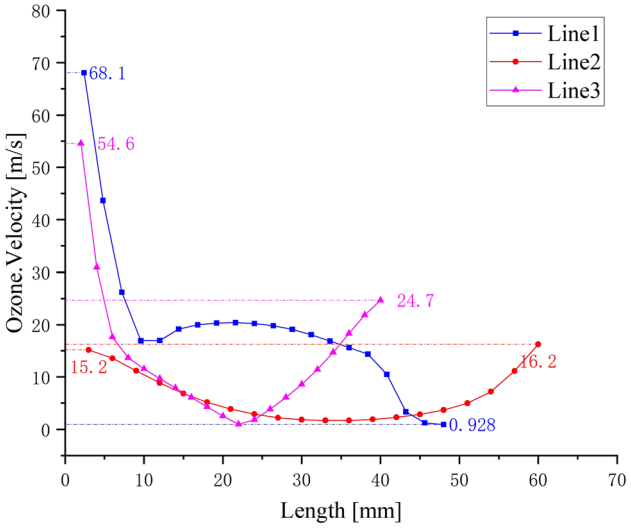

Figure 6: Curves of the ozone velocity varying with the length of three lines.

3 Results and discussion

The position of ozone entrance is located at the upper side 30 mm from the left chamber surface to conduct numerical analysis of the chemical reaction of ozone decomposition in the chamber with self-excitation pulse. A set of nozzle parameters that can produce a self-excited pulse effect is selected as the basic working condition setting [33]. The structural parameters are set as shown in Table 3 [25]. To compare and analyze the efficiency of ozone degradation, there are three collision angles to be set in this study.

3.1 Collision angle of 120°

Figures 8 and 9 are, respectively, the contours of ozone mass fraction distribution and oxygen mass fraction distribution in the chamber, at four representative reaction moments, during the ozone degradation process, and the collision angle is 120°.

It can be seen that ozone did not degrade in the self-excited pulse cavity chamber, and there is no oxygen in Figure 9. With the cavitation reaction occurring in the chamber, ozone degrades under the action of the cavitation jet, and oxygen begins to be generated gradually. The rate of oxygen production is positively correlated with ozone degradation. Ozone degrades near the wall, where cavitation collapse occurs, and then gradually diffuses throughout the chamber. It is also where oxygen is first produced and then permeates the whole chamber. In the process of simulation, the inflow of ozone is continuous. When most of the generated oxygen is jetted out with the water jet from the outlet of the lower nozzle, the residual ozone and newly introduced ozone in the chamber continue the above series of reactions, and there may be residual oxygen in the chamber, whether it affects the subsequent ozone degradation needs to be further verified.

3.2 Collision angle of 180°

The structure parameters were kept unchanged, the ozone inlet flow was still set at 20 g/h, and the impact angle was

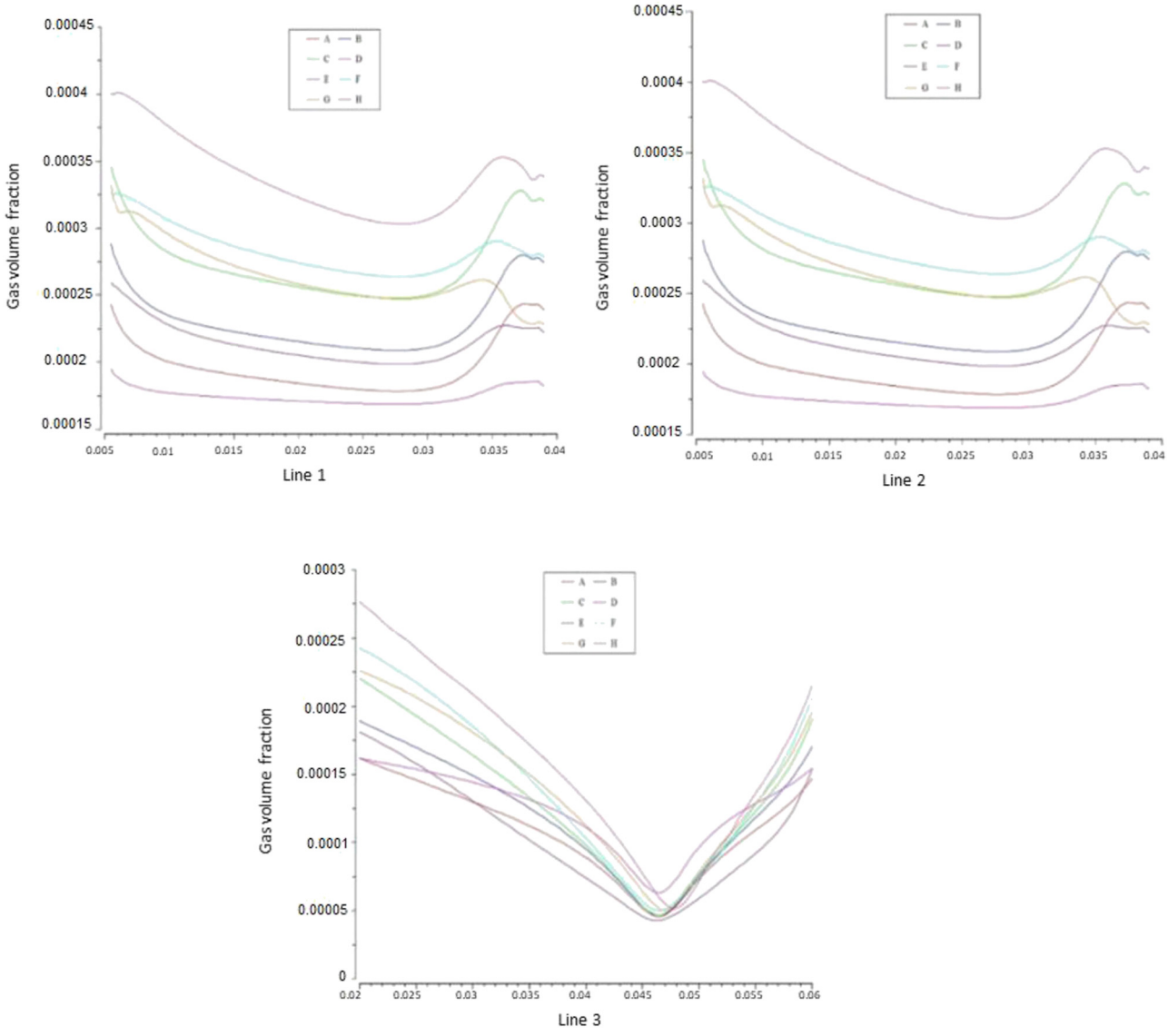

Figure 7: Data processing diagram of the three-line method.

Table 3: Structural parameters

d_1	d_2	L	D	θ (°)
5 mm	11 mm	50 mm	78 mm	90 120 180

changed to 180°. Then, the changes in chemical reactions in the chamber under the impact angle of 180° were analyzed. Figures 10 and 11, respectively, show the distribution of ozone mass fraction and oxygen mass fraction in the chamber during the process of ozone degradation when the collision angle is 180°.

From Figures 10 and 11, it can be seen that when the collision angle is 180°, the ozone decomposition and oxygen generation process in the whole chamber is the same as that under the collision angle of 120°. Ozone decomposition and oxygen generation occur near the impact surface and the wall surface and then spread to the whole chamber. However, there is a certain difference in chemical reaction intensity and oxygen generation. It was found that the cavitation reaction in the chamber of self-excited pulse chamber at the collision angle of 180° is more violent than that at 120°. Similarly, the ozone decomposition reaction at this angle is also more violent, and the oxygen production is also more than that at 120°, indicating that the ozone degradation rate has been improved to a certain extent at the collision angle of 180°.

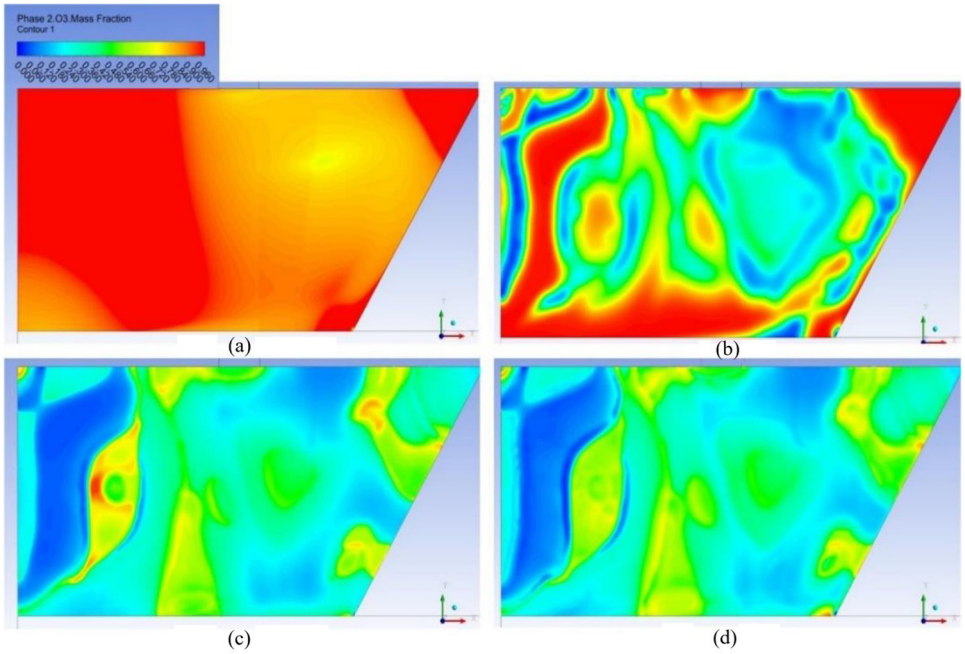

Figure 8: Contours of ozone mass fraction at 120°. (a) $t = T/4$, (b) $t = T/2$, (c) $t = 3T/4$, and (d) $t = T$.

3.3 Collision angle of 90°

While the parameters and boundary conditions are kept unchanged, the minimum collision angle 90° is used for the final chemical reaction numerical simulation analysis. Figures 12 and 13, respectively, show the distribution cloud map of ozone mass fraction and oxygen mass fraction in the chamber during the process of ozone degradation at 90°.

In Figures 12 and 13, when the impact angle is 90°, the process of ozone decomposition and oxygen generation in the whole chamber is the same as that under the impact angles of 120° and 180°. However, when the

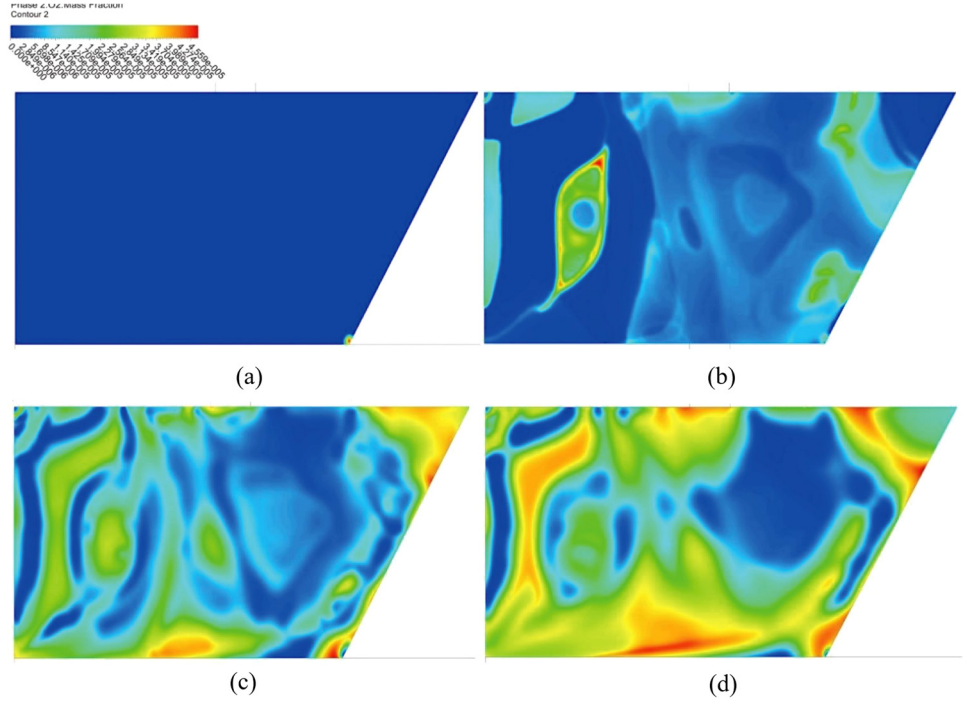

Figure 9: Contours of oxygen mass fraction at 120°. (a) $t = T/4$, (b) $t = T/2$, (c) $t = 3T/4$, and (d) $t = T$.

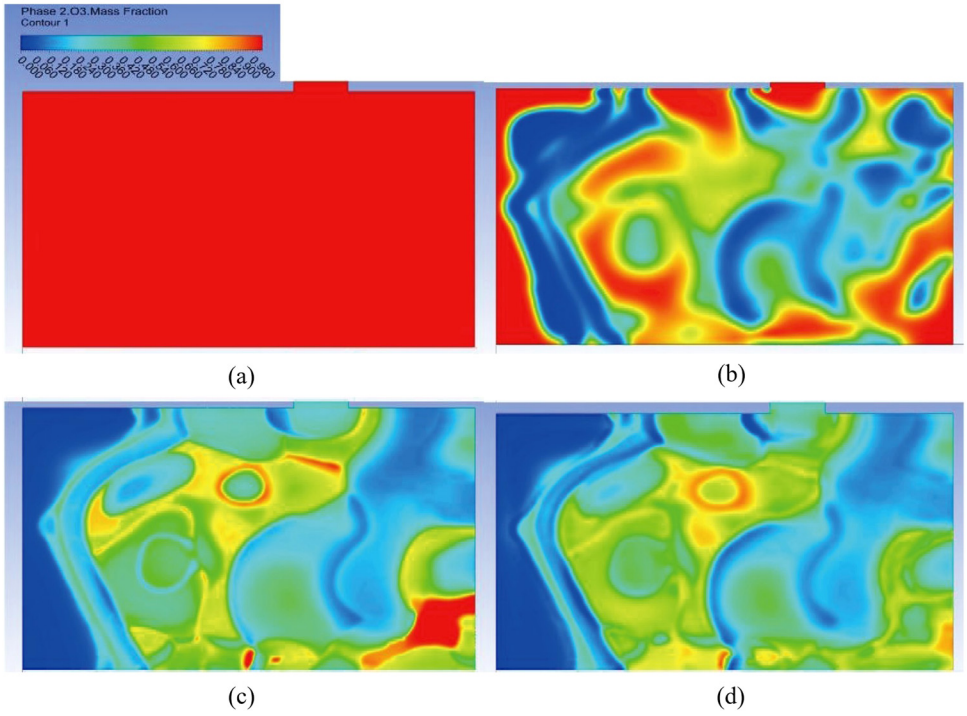

Figure 10: Contours of ozone mass fraction at 180°. (a) $t = T/4$, (b) $t = T/2$, (c) $t = 3T/4$, and (d) $t = T$.

collision angle is 90°, the upper left corner of the impact surface can hardly be impacted due to the small angle of jet flow, so ozone degradation is very difficult to occur. There is also a certain difference in chemical reaction intensity and oxygen production. The cavitation reaction in the chamber of the self-excited pulse at 90° collision angle is relatively mild compared with that of 120° and 180°. The ozone decomposition reaction at this angle is

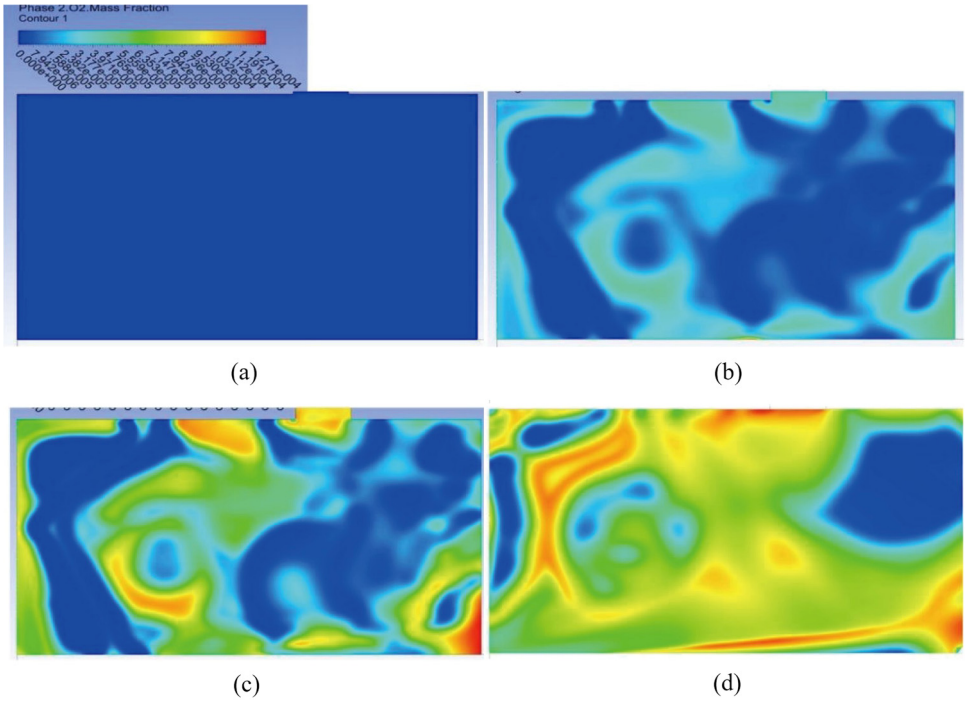

Figure 11: Contours of oxygen mass fraction at 180°. (a) $t = T/4$, (b) $t = T/2$, (c) $t = 3T/4$, and (d) $t = T$.

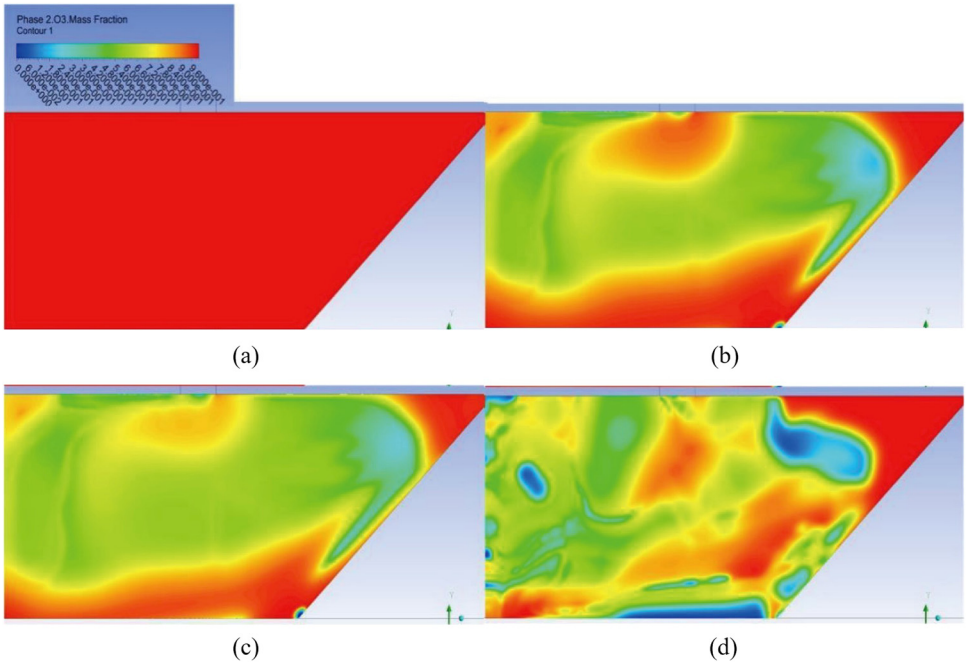

Figure 12: Contours of ozone mass fraction at 90°. (a) $t = T/4$, (b) $t = T/2$, (c) $t = 3T/4$, and (d) $t = T$.

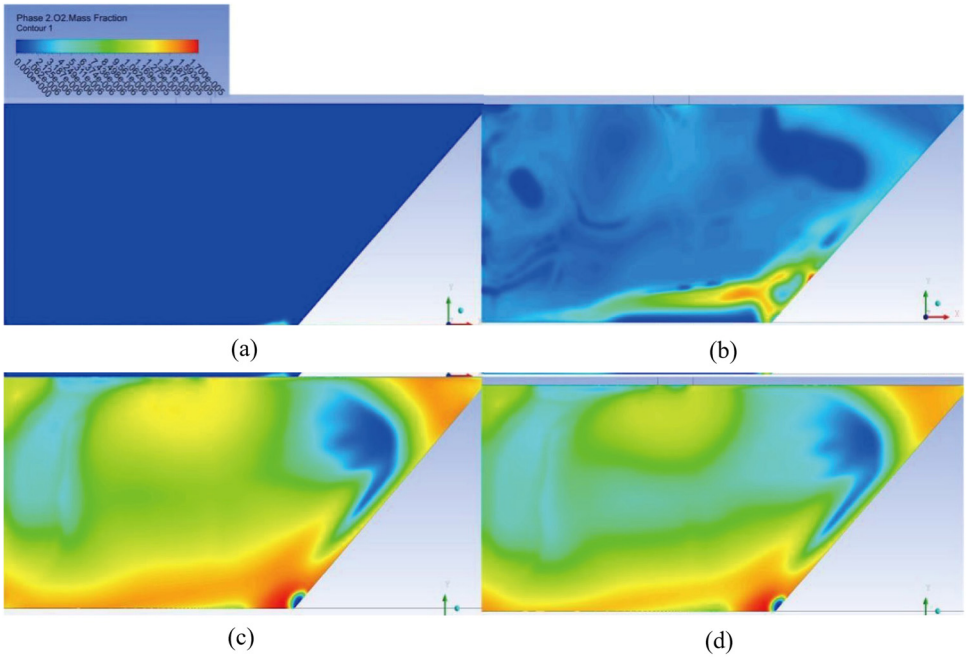

Figure 13: Contours of oxygen mass fraction at 90°. (a) $t = T/4$, (b) $t = T/2$, (c) $t = 3T/4$, and (d) $t = T$.

also relatively low, and the oxygen production is relatively low, indicating that the ozone degradation rate at the collision angle of 90° is lower than before, preliminarily indicating that this collision angle may not be suitable for chemical reaction.

4 Conclusion

In this study, based on the summary of the mechanism of ozone in aqueous solution and the degradation mechanism of self-excited pulsed cavitation jet, the ozone degradation

under different collision angles was discussed using the numerical simulation.

With the occurrence of cavitation reaction in the jet chamber, ozone degradation occurs, and oxygen begins to generate gradually. There is a positive correlation between oxygen generation rate and ozone degradation. At the same time, degradation occurs first near the wall, that is, the place where cavitation and collapse occur.

From the simulation results of ozone degradation and oxygen generation under different collision angles, it is found that different collision angles have a certain influence on the intensity of chemical reaction, which affects the amount of ozone degradation and oxygen generation. The chemical reaction is the most violent at the collision angle of 180°, the ozone degradation and oxygen generation are the most at 120°, and least at 90°.

Funding information: This work was supported by the National Natural Science Foundation of China (52006126), the Fundamental Research Funds of Shandong University (2018GN033) and Key Laboratory of High-efficiency and Clean Mechanical Manufacture at Shandong University, Ministry of Education, and the Ocean industry-leading talent team of Yantai's Double Hundred Plan, and the Key Research and Development Project of Shandong Province (2019GGX102058).

Author contributions: All authors have accepted responsibility for the entire content of this manuscript and approved its submission.

Conflict of interest: The authors state no conflict of interest.

Data availability statement: The data that support the findings of this study are available from the corresponding author upon reasonable request.

References

[1] Yi C, Li G, Shen Z. Experimental study on drilling rate improvement by self-resonating cavitating jet. Nat Gas Ind. 2006;26(5):52–4.
[2] Qu Y, Chen S. Orthogonal experimental research on the structural parameters of a self-excited pulsed cavitation nozzle. Eur J Mech B-Fluids. 2017;65:179–83.
[3] Wang P, Ma F. Vibration analysis experiment of self-resonating cavitating water jet. Chin J Mech Eng. 2009;45(10):89–95.
[4] Qu Y, Zhou C, Zhong Y, Chen S, Wang R. A computational study on gas-liquid flow in a lime slurry pond equipped with a rotary jet mixing system. Adv Mech Eng. 2017;9(2):168781401769046.
[5] Wang R, Wang H, Chen S, Qu Y, Wang C. Numerical investigation of multiphase flow in flue gas desulphurization system with rotary jet stirring. Results Phys. 2017;7:1274–82.
[6] Hu T. Study on the cavity bubble motion characteristics of low-pressure self-excited pulse cavitation jet. [Thesis for Master degree]. Jinan: Shandong University; 2014.
[7] Sun J, Xiang L, Wei X, Chen S. Study on different line gasoline blending with RJM via numerical investigation. Results Phys. 2019;12:1285–90.
[8] Chen S, Li C, Qu Y. Research on the effect factors of the novel self-excited oscillation pulse jet. J Shandong Univ (Eng Sci). 2006;36(4):12–5.
[9] Moholkar VS, Pandit AB. Bubble behavior in hydrodynamic cavitation: effect of turbulence. Aiche J. 1997;43(6):1641–8.
[10] Sun X, Chen S, Liu J, Zhao S, Yoon JY. Hydrodynamic cavitation: a promising technology for industrial-scale synthesis of nanomaterials. Front Chem. 2020;8:259.
[11] Kalumuck KM, Chahine GL. The use of cavitating jets to oxidize organic compounds in water. J Fluids Eng-Transactions Asme. 2000;122(3):465–70.
[12] Jyoti KK, Pandit AB. Water disinfection by acoustic and hydrodynamic cavitation. Biochem Eng J. 2001;7(3):201–12.
[13] Sun X, Liu J, Ji L, Wang G, Zhao S, Yoon JY, Chen S. A review on hydrodynamic cavitation disinfection: the current state of knowledge. Sci Total Environ. 2020;737:139606.
[14] Chakinala AG, Gogate PR, Burgess AE, Bremner DH. Treatment of industrial wastewater effluents using hydrodynamic cavitation and the advanced Fenton process. Ultrason Sonochem. 2008;15(1):49–54.
[15] Yao P, Zheng H, Yang J. Study on the decomposition of ozone in the air coefficient. Energy, Environ Sustain Ecosyst Dev. 2016;13:603–13.
[16] Trapido M, Veressinina J, Munter R. Ozonation and AOP treatment of phenanthrene in aqueous-solutions. Ozone-Sci Eng. 1994;16(6):475–85.
[17] Staehelin J, Hoigne J. Decomposition of ozone in water in the presence of organic solutes acting as promoters and inhibitors of radical chain reactions. Environ Sci Technol. 1985;19(12):1206–13.
[18] Gracia R, Aragues JL, Ovelleiro JL. Mn(II)-catalysed ozonation of raw Ebro river water and its ozonation by-products. Water Res. 1998;32(1):57–62.
[19] Mainardis M, Buttazzoni M, De Bortoli N, Mion M, Goi D. Evaluation of ozonation applicability to pulp and paper streams for a sustainable wastewater treatment. J Clean Prod. 2020;258:120781.
[20] Zhai L, Dong S, Feng G, Ma H. Experimental study on hydrodynamic cavitation and ozone in degrading oilfield wastewater. Sci Technol Rev. 2009;27(6):38–42.
[21] Chang J, Fan J, Wang W, Zhao L, Shao L. Advanced treatment of semi-coking wastewater by ozonation in rotating packed bed. Environ Prot Chem Ind. 2020;40(2):131–6.
[22] Yang W, Zhang Y, Li W, Xu T, Wang W. Experiment of processes of hydrodynamic cavitation combined with ozonation for resin production wastewater treatment. Water Purif Technol. 2017;36(03):90–5.
[23] Hui H. Application progress of ozone oxidation technology in water treatment. Ind Water Wastewater. 2019;50(02):6–9.
[24] Zhang J, Qu K, Ma SUV. Irradiation technique and its application to aquaculture. Mar Fish Res. 2006;27(1):93–7.

[25] Wang J, Li J, Guan K. Experimental study of self-excited pulse jet. J Eng Thermophys. 2014;35(4):678–81.
[26] Kumar PS, Kumar MS, Pandit AB. Experimental quantification of chemical effects of hydrodynamic cavitation. Chem Eng Sci. 2000;55(9):1633–9.
[27] Phelps AV. The diffusion of charged-particles in collisional plasmas-free and ambipolar diffusion at low and moderate pressures. J Res Natl Inst StTechnol. 1990;95(4):407–31.
[28] Wang Z. Cavitation characteristics study on the outlet channel of atomization nozzle based on the self-excited oscillating pulse effects. J Mech Eng. 2016;52(14):204–12.
[29] Wang Z, Chen S, Deng X. Research on modified cavitation model for self-excited oscillation pulsed jet nozzle. International Conference on Mechanical, System and Control Engineering (ICMSC); 2017. p. 90–5.
[30] Zhou Z, Ge Z, Lu Y, Zhang X. Experimental study on characteristics of self-excited oscillation pulsed water jet. J Vibroengineering. 2017;19(2):1345–57.
[31] Eliasson B. Basic data for modeling of electrical discharges in gases: oxygen. Asea Brown Boveri Corporate Research Report; 1986. p. KLR86-11C.
[32] Freisinger B, Kogelschatz U, Schafer JH, Uhlenbusch J, Vil W. Ozone production in oxygen by means of F2-laser irradiation at λ = 157.6 nm. Appl Phys B, Photophysics Laser Chem. 1989;49(2):121–9.
[33] Xiang L, Wei X, Chen S. Experimental study on the frequency characteristics of self-excited pulsed cavitation jet. Eur J Mech B Fluids. 2020;83:66–72.